Earthquake Geotechnical Engineering for Protection and Development of Environment and Constructions – Silvestri & Moraci (Eds)
© 2019 Associazione Geotecnica Italiana, Rome, Italy, ISBN 978-0-367-14328-2

Simultaneous effect of uplift and soil-structure interaction on seismic performance of storage tanks

D. Hernandez-Hernandez, T. Larkin & N. Chouw
The University of Auckland, Auckland, New Zealand

ABSTRACT: Tanks are often founded on weak compressive soil due to their proximity to a harbour and rivers. This soil condition carries with it a strong probability of significant soil-structure interaction including uplift under earthquake loading. This paper evaluates the seismic response of a tank, and the kinematics including uplift and forces that evolve from strong seismic response. To simulate the near-surface shear deformations of soil, a laminar box on a shake table was used. The work highlights the difference between stresses developed in a tank wall for three base cases: 1) fixed-base tank to a rigid base, 2) unanchored tank on a rigid base and 3) tank on sand free to uplift. Results reveal that stresses of the free-base conditions are significantly larger in magnitude than those from the fixed-base condition. Furthermore, a flexible soil condition reduces maximum uplift by 50%. Thus, maximum hoop and axial stresses also decrease.

1 INTRODUCTION

Liquid storage tanks are utilized to store water, petrol or other chemicals. In emergencies, e.g. after a strong earthquake, their integrity is a key factor in the rate of recovery of the affected communities. However, past experiences with strong earthquakes have shown the complex behaviour of tanks under dynamics loads.

Damage to storage tank walls are usually associated with high concentration of both hoop and axial stress. Hoop stress is related to the hydrodynamic pressure due to the liquid. Axial stress is normally associated with uplift, which is the transient separation of a part of the tank base from the supporting foundation. Because tanks are generally built near to harbours and rivers where the predominant soil has low compressive resistance, another factor that may boost the tank response is the soil-structure interaction (SSI).

SSI involves many variables that have not been addressed in a holistic design so far. The majority of studies in this subject has been numerical but opinions disagree on some of the key parameters of SSI. For instance, Cho et al. (2004), Haroun & Abou-lzzeddine (1992), and Veletsos & Tang (1990) claim that a flexible support condition is beneficial to the tank response, i.e. the magnitude of acceleration and stresses are reduced. Larkin (2008) ascertained that tank response reduction depends on the soil and tank properties, making emphasis on the changes that natural frequency of the tank-soil system may suffer. If a natural frequency of the tank is close enough to the predominant frequency of the soil site, an amplification in the response may occur (Daysal & Nash 1984, Durmus & Livaoglu 2015 and Ma & Chang 1993). Hence, during the design phase, assuming a rigid support condition does not always guarantee conservative results (Seeber et al. 1990).

A few experimental-based studies have been conducted considering SSI (Hori 1987; Ormeño et al. 2012, 2013a, 2013b). Ormeño et al. (2013b) utilized a PVC tank on a shake table, focusing on the development of axial stresses. To simulate a flexible base support, a rigid box with sand was utilised. Overall, it was concluded that SSI leads to a significant reduction in axial and hoop stresses, but that the reduction is very sensitive to the water level inside the tank.

The present paper evaluates, through an experimental study using a laminar box and a unidirectional shake table, the combined effects of uplift and a flexible foundation on the earthquake-induced stresses in a tank wall. Only a horizontal component of the earthquake is utilised.

2 EXPERIMENTAL METHODOLOGY

2.1 *Tank model*

A low-density polyethene (LDPE) tank, 450 mm in diameter and 750 mm in height, is used to model a prototype steel tank. The similitude conditions may be defined using the Buckingham π theorem, along with the Cauchy number for a Single-Degree-of-Freedom (SDOF) system (Qin et al. 2013). Neglecting the influence of oscillations at the fluid free surface, i.e. the convective mode of response, the model can be analysed as a SDOF system based only on the impulsive inertia forces on the tank wall (Veletsos & Tang 1990). The model and prototype properties are shown in Table 1 and the scale factors are shown in Table 2. The fundamental periods were estimated according to the NZSEE (2009).

Two support conditions for the tank were utilised: 1) the tank sitting on a rigid steel plate fixed to the shake table to represent a rigid support condition, i.e. tank on rock, Figures 1a and 2) the tank on sand contained in a laminar box (described in Section 2.4) i.e. a flexible support condition representing a soil site, Figure 1b. All tests were performed with a liquid height of 675 mm, which corresponds to an aspect ratio of three. Three tank base conditions are compared: 1) the tank is fixed to the rigid steel plate, 2) the tank is unanchored and is placed directly on the rigid steel plate and 3) the tank is resting freely on sand in the laminar box.

2.2 *Set-up*

Three columns of strain gauges (0°, 90° and 180°) were attached to the external face of the LDPE container, see Figure 1c. At each height, two strain gauges are employed, one to evaluate hoop stress (circumferential direction) and one to evaluate the axial stress, in the x-axis direction. In both foundation support cases (rigid and flexible) an accelerometer was attached to the shake table. In order to obtain the axial σ_x and hoop σ_ϕ stress on the surface of the shell of the tank, it is necessary to combine the data from two strain gauges at each height, according to Equations (1) and (2) (Flügge 1973).

$$\sigma_x = \frac{E}{1-\nu^2}(\epsilon_x + \nu \in_\phi) \tag{1}$$

$$\sigma_\phi = \frac{E}{1-\nu^2}(\epsilon_\phi + \nu \in_x) \tag{2}$$

Table 1. Properties of the model and prototype.

Material	LDPE Model	Steel prototype
Young's Modulus (Pa)	1.12×10^9	2.1×10^{11}
Radius (m)	0.225	4.5
Height (m)	0.675	13.5
Liquid mass (kg)	107	858 833
Impulsive period T(s)	0.066	0.143

Table 2. Scale factors.

Dimension	Scale factors
Length	20
Mass	8000
Time	2.17
Acceleration	4.25

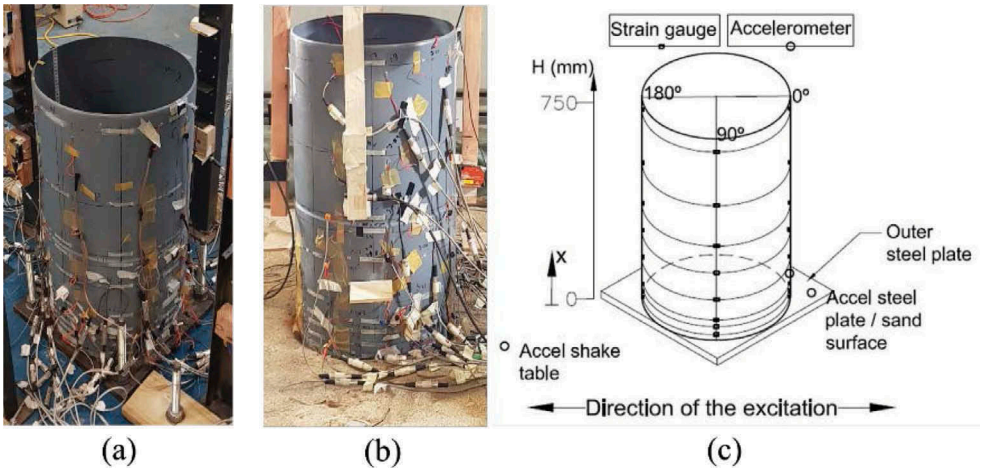

Figure 1. LDPE tank (a) fixed-rigid base (b) free-flexible base (c) measurement locations.

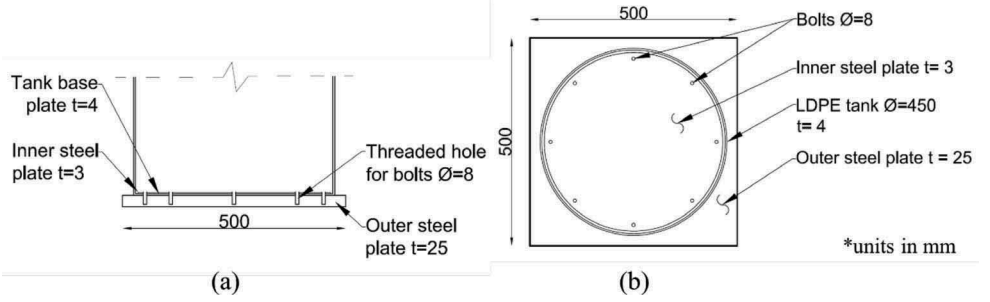

Figure 2. Base restriction for the LDPE tank. (a) Frontal view, and (b) top view.

where E is the modulus of elasticity; Poisson's ratio, experimentally determined by tensile test is $\nu = 0.41$; ϵ_x axial strain; ϵ_ϕ hoop strain.

2.3 *Anchorage*

The LDPE tank was fixed to a rigid steel plate of 25 mm thickness through eight bolts = 8 *mm*. A round steel plate 3 mm thickness was allocated inside the tank to avoid stress concentration on the base plate due to the bolts pressure, as shown in Figure 2. Hence, modifications to the tank wall stiffness were avoided. An extra accelerometer was placed on the steel plate to record the acceleration at the tank base (see Figure 1c).

2.4 *Laminar box*

A 2 m cubic laminar box is used to simulate the earthquake-induced shear deformation of the sand due to the shake table motion (Figure 3). The maximum displacement of each layer of the laminar box is 175 mm in the horizontal direction. More information regarding the characteristics of the box can be found in Qin & Chouw (2017). The box is filled to a height of 1.43 m with sand with an average density of 1.58 t/m^3. One accelerometer was on the sand surface to measure the real acceleration at the tank base.

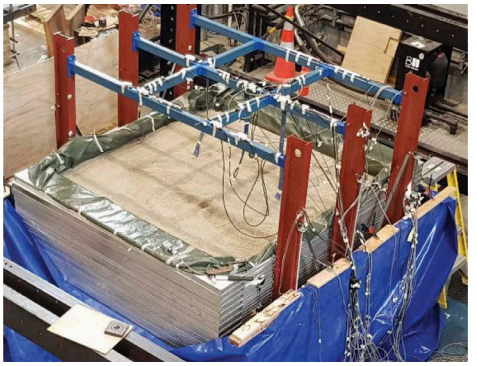

Figure 3. Cubic laminar box filled with sand.

The shear wave velocity was measured at the beginning of the experiment by performing an impulse test, to ascertain the shear stiffness of the sand. The set-up and the recorded accelerations are shown in Figure 4. A circular steel plate was placed on the sand surface and hit by a hammer. The impact produces a downward travelling shear wave that was recorded by two accelerometers with a distance 700 mm apart. The average shear wave velocity v_{sm} may be estimated by dividing the travel distance ΔL by the travel time Δt. From Figure 4, the travel time is $\Delta t = 1.1554 - 1.1514 = 0.004\ s$. The estimated mean velocity is

$$v_{s_m} = \frac{0.70}{0.004} = 175 \frac{m}{s}$$

An empirical method to estimate the shear wave velocity is by Equation (3) (Larkin 1978):

$$v_s = \sqrt{\frac{D_r + 25}{100}} \sqrt{\frac{0.422 \times 10^6 \left(\sigma'_m\right)^{\frac{1}{2}}}{\rho}} \tag{3}$$

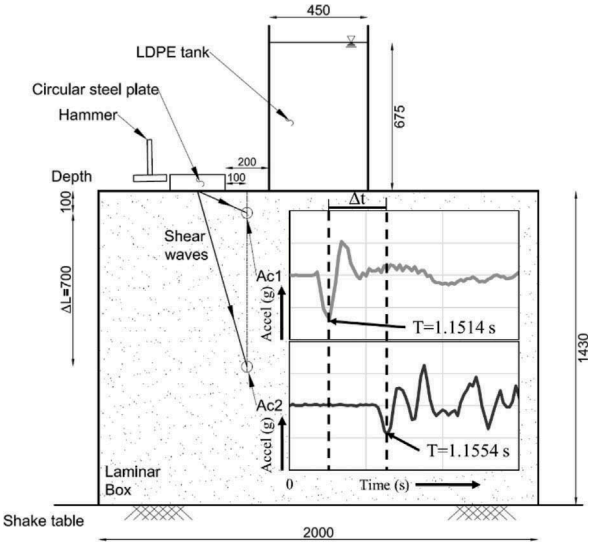

Figure 4. Configuration of impulse test and shear waves recorded by both accelerometers (units in mm).

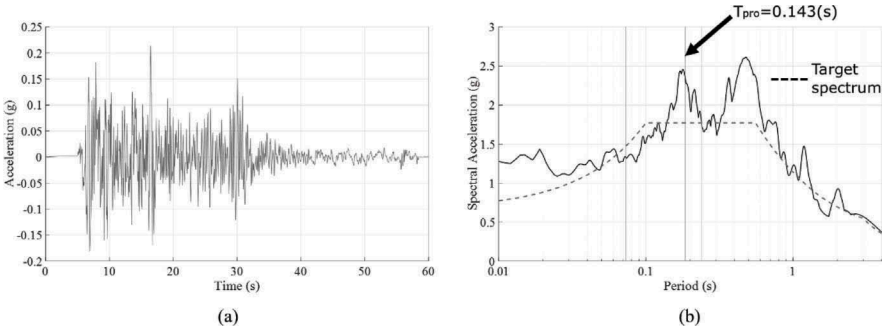

Figure 5. Ground excitation. (a) El Centro earthquake scaled and (b) response spectrum of El Centro earthquake and target spectrum for a soft soil condition defined by NZS 1170.5.

where D_r is the sand relative density, $D_r = 56\%$; ρ is the sand mass density, 1580kg/m^3; σ'_m is the mean stress at the respective depth, estimated as $\sigma'_m = (\sigma'_v + 2\sigma'_h)/3$; σ'_v is the effective vertical stress and σ'_h is the horizontal effective stress.

The stresses may be estimated by elastic solutions for a uniform surface circular stress, in this case 675 kPa. This gives estimates of the mean stress as:

$$\sigma'_{m_{100}} = 405\ Pa; \quad \sigma'_{m_{800}} = 135\ Pa$$

Hence, the shear wave velocity is:

$$\nu_{s_{100}} = 222\frac{m}{s}; \quad \nu_{s_{800}} = 169\frac{m}{s}; \quad \nu_{s_m} = 196\frac{m}{s}$$

The subscript numbers indicate the depth from the sand surface and "m" indicates the mean value. The estimated mean shear wave velocity is similar to the result obtained experimentally.

2.5 *Excitation applied*

The acceleration recorded from El Centro earthquake (1940), Figure 5a was used as input for the shake table. The target spectrum was calculated following the NZSEE recommendations for time-domain analysis of liquid storage tanks (NZS 1170.5 2004; NZSEE 2009) for a soft soil condition, classification D. To avoid any underestimation of stresses, the lower limit of frequency given by the NZS 1170.5 for storage tanks was ignored in this work (Ormeño et al. 2015). Hence, the lower limit applied is 0.4 T_{pro} = 0.057 *s* and the upper limit is 1.3 T_{pro} = 0.186 *s*. The response spectrum of the El Centro earthquake and the target spectrum are shown in Figure 5b. The range of period of interest $[0.057,\ 0.186]s$ for matching the response spectrum, following the scaling method of NZS 1170.5 (2004), and the natural period of vibration of the tank with an assumed fixed base are shown.

3 RESULTS

Figure 6 shows the acceleration at the tank base for the three base conditions. For a fixed and free rigid base condition, the maximum acceleration at the tank base is similar. However, the maximum acceleration on the sand surface is five times larger of that on the rigid base. Due to this amplification, the maximum axial and hoop stress are expected to be larger when the tank is resting on sand than those when the tank is on the steel plate.

Making a zoom of Figure 6 for time $t = [13, 16]s$, where the maximum acceleration occurred, Figures 7a-b show the time-history of the absolute value of hoop and axial stresses

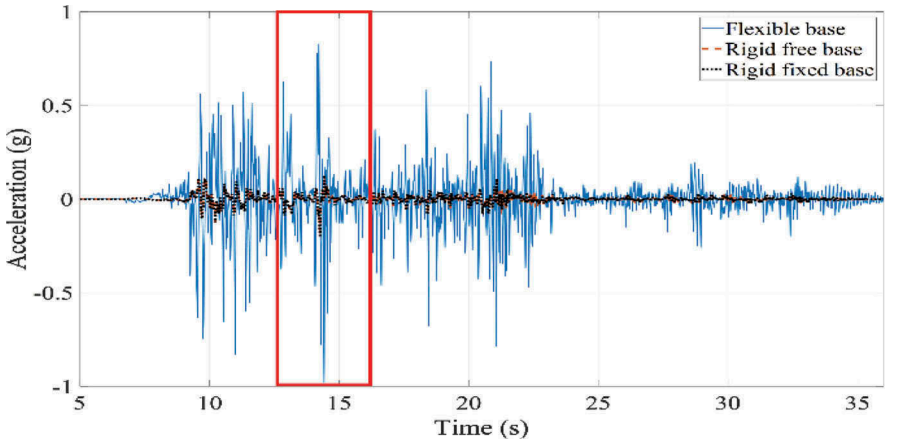

Figure 6. Time-history acceleration at the tank base for the three base conditions.

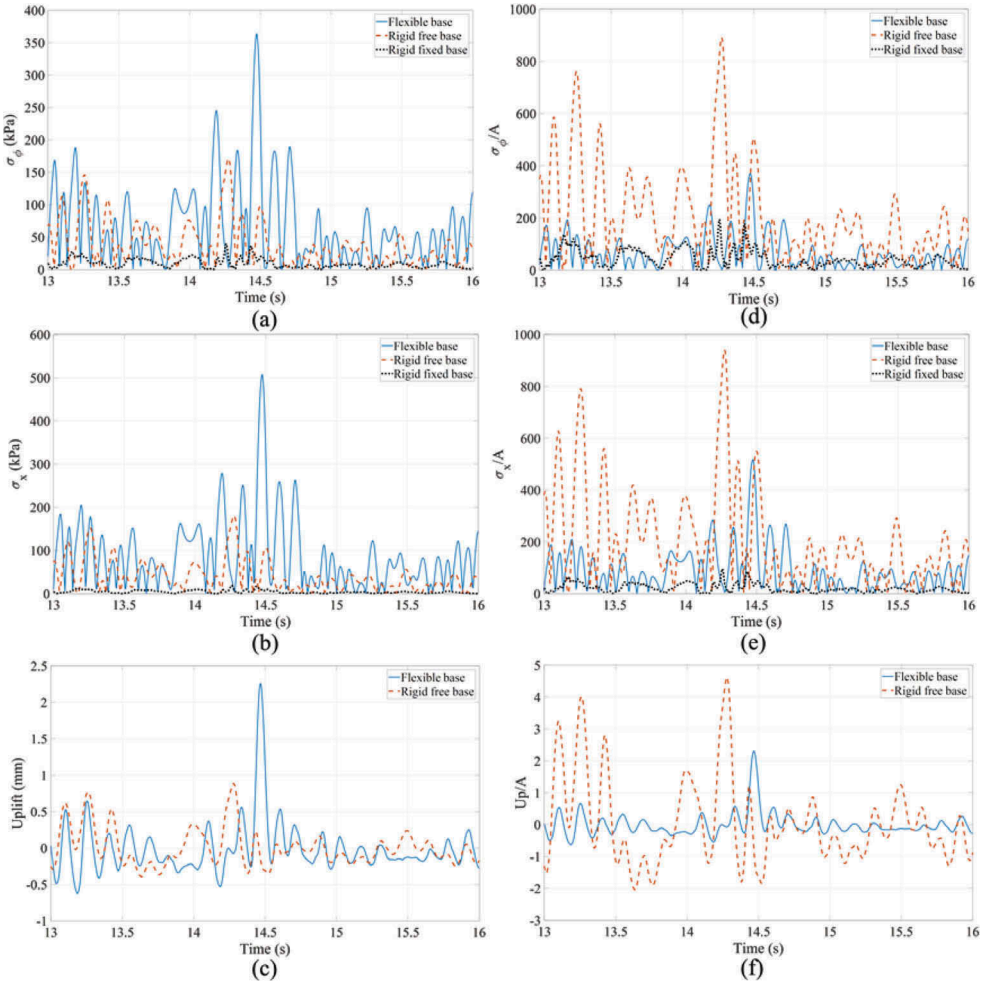

Figure 7. Comparison of results of the three base conditions for the time t = [13,16] s. (a) Hoop stress, (b) axial stress, (c) uplift, (d) normalized hoop stress, (e) normalized axial stress and (f) normalized uplift.

Table 3. Maximum absolute magnitude of acceleration, hoop stress, axial stress and uplift for the three base conditions.

Support condition				Rigid				Flexible		
Base condition		Fixed	Time	Delay	Free	Time	Delay	Free	Time	Delay
			(s)	(s)		(s)	(s)		(s)	(s)
A (g)	Shake table	0.19	14.25	–	0.20	14.26	–	0.19	14.29	–
	Tank base	0.19	14.25	0	0.20	14.26	0	0.98	14.42	0.13
Stress	Hoop	39	14.26	0.01	171	14.28	0.02	364	14.48	0.19
(kPa)	Axial	19	14.26	0.01	181	14.28	0.02	507	14.48	0.19
Uplift (mm)		–	–	–	0.87	14.28	0.02	2.26	14.47	0.18

for the column of 0° that is co-linear with the motion of the shake table. Those stresses are calculated employing Equations 1 and 2, using the data from the strain gauges at 20 mm from the base. Figure 7c shows the uplift time-history for both flexible and rigid base conditions. As expected, axial and hoop stresses and uplifting are larger in magnitude when the tank is resting on sand than those when the tank is on the steel plate.

However, to assess the influence of the flexible soil, those results are normalized respect to the maximum acceleration at the tank base for each case. Figures 7d-f show that the most unfavourable condition is when the tank is resting freely on a rigid base. The maximum values of acceleration, stress and uplift and the time when they occurred are summarized in Table 3. The delay between the maximum acceleration, stress and uplift are also shown.

Comparing the maximum stresses for the three cases, the maximum absolute hoop stress on the free rigid base is three times larger than those from the fixed base condition. For the axial stress, the free base condition is even more unfavourable, i.e. the magnitude of the stress increases ten times. Comparing the normalized results of flexible and rigid base conditions, hoop and axial stress decreased by 240% and 180%, respectively, when the tank is resting on sand.

Regarding the magnitude of uplift, it is reduced by half compared with that when the tank is free on a rigid base condition. Thus, uplift is significantly influencing the magnitude of stresses for both rigid and flexible base. For this particular earthquake, maximum absolute axial stresses are higher in magnitude than hoop stresses, except when the tank is fixed to a rigid base.

For the rigid base case, there is an unnoticeable delay between the acceleration of the shake table and the acceleration at the tank base (0.01 *s* and 0.02 *s*). Hence, the maximum stresses and uplift occurred exactly at the same time. Conversely, a delay between the acceleration of the shake table and the acceleration on the sand surface is noted. For the maximum acceleration, the delay is 0.13*s*, then after a five centiseconds, the maximum uplift occurred and it is producing the maximum hoop and axial stress, one centisecond later.

4 CONCLUSIONS

A low-density polyethylene tank has been tested under three different base conditions using a shake table and a laminar box: 1) Fixed base on a rigid foundation (the shake table), 2) free base on a rigid foundation and 3) free base on a flexible foundation (sand). The tank was tested full of water. The main objective was to evaluate the combined effects of the flexible foundation medium and uplift on the maximum hoop and axial stresses in the tank wall. The results from the experiments reveal:

Uplift increases the maximum hoop stress by four times and the maximum axial stress by nearly ten times compared to the case when the tank is fixed to a rigid base. For a flexible support condition, the maximum hoop stress increases by four times and axial stress by two times when compared to the fixed base condition.

The sand in the laminar box amplify the acceleration at the tank base and, consequently, the stresses and uplift are larger in magnitude than those from the tank resting freely on a rigid base. However, if the results are normalized respect to the maximum acceleration at the base of the tank, SSI reduces by 50% the maximum uplift compared to that when the tank is resting freely on a rigid base. Hence, the maximum hoop stress and axial stress decrease by 240% and 180%, respectively.

For El Centro earthquake, the axial stress is larger in magnitude than the corresponding hoop stress at the same height, when uplift occurs. Those results suggest that for unanchored tanks, axial stress should be used to design the ultimate resistance of the tank.

REFERENCES

Cho, K.H., Kim, M.K., Lim, Y.M. & Cho, S.Y. 2004. Seismic response of base-isolated liquid storage tanks considering fluid-structure-soil interaction in time domain. *Soil Dyn. Earthq. Eng*. 24, 839–852. https://doi.org/10.1016/j.soildyn.2004.05.003

Daysal, H. & Nash, W.A. 1984. Soil structure interaction effects on the seismic behavior of cylindrical liquid storage tanks, in: Eighth World Conference on Earthquake Engineering. San Francisco, California, 21–28 July.

Durmus, A. & Livaoglu, R. 2015. A simplified 3 DOF model of a FEM model for seismic analysis of a silo containing elastic material accounting for soil-structure interaction. *Soil Dyn. Earthq. Eng*. 77, 1–14. https://doi.org/10.1016/j.soildyn.2015.04.015

Flügge, W. 1973. *Stresses in Shells*, Second Edi. ed, Springer-Verlag.

Haroun, M.A. & Abou-lzzeddine, W. 1992. Parametric study of seismic soil-tank interaction. I: Horizontal excitation. *J. Struct. Eng*. 118, 783–797.

Hori, N. 1987. Effects of soil on the dynamic response of liquid-tank systems. *Am. Soc. Mech. Eng. Press. Vessel. Pip. Div*. PVP 127, 339–347. https://doi.org/10.1115/1.2928596

Larkin, T. 2008. Seismic response of liquid storage tanks incorporating soil structure interaction. *J. Geotech. Geoenvironmental Eng*. 134, 1804–1814.

Larkin, T. 1978. Report N° 51508/6. Oslo, Norwey.

Ma, L. & Chang, C.S. 1993. Pressures exerted on soil due to rocking of liquid storage tanks. *J. Geotech. Eng*. 119, 1679–1695. https://doi.org/10.1061/(ASCE)0733-9410(1993)119:11(1679)

New Zealand Standard NZS1170.5 2004. Structural design actions, Part 5: Earthquake actions - New Zealand.

NZSEE 2009. Seismic design of storage tanks, 2009: Recommendations of a study group of the New Zealand Society for Earthquake Engineering. New Zealand Society for Earthquake Engineering, Wellington.

Ormeño, M., Larkin, T. & Chouw, N. 2015. Evaluation of seismic ground motion scaling procedures for linear time-history analysis of liquid storage tanks. *Eng. Struct*. 102, 266–277. https://doi.org/10.1016/j.engstruct.2015.08.024

Ormeño, M., Larkin, T. & Chouw, N. 2013a. Effect of foundation conditions on the seismically induced stresses of liquid storage tanks, in: 2013 NZSEE Conference. Welligton, New Zealand, 26–28 April.

Ormeño, M., Larkin, T. & Chouw, N. 2013b. Effects of subsoil on seismic wall stresses in liquid storage tanks: Experimental findings, in: Orense, R., Tohwate, I., Chouw, N. (Eds.), New Zealand-Japan Workshop on Soil Liquefaction during Recent Large-Scale Earthquakes. CRC Press, the University of Auckland, pp. 233–240.

Ormeño, M., Larkin, T. & Chouw, N. 2012. Influence of uplift and SSI on liquid storage tanks during earthquakes, in: 15th World Conference on Earthquake Engineering. Lisboa, Portugal, 24–28 September.

Qin, X., Chen, Y. & Chouw, N. 2013. Effect of uplift and soil nonlinearity on plastic hinge development and induced vibrations in structures. *Adv. Struct. Eng*. 16, 135–147. https://doi.org/10.1260/1369-4332.16.1.135

Qin, X. & Chouw, N. 2017. Shake table study on the effect of mainshock-aftershock sequences on structures with SFSI. *Shock Vib*., 1–12. https://doi.org/10.1155/2017/9850915

Seeber, R., Fischer, F.D. & Rammerstorfer, F.G. 1990. Analysis of a three-dimensional tank-liquid-soil interaction problem. *Trans. ASME*, 112, 28–33.

Veletsos, A.S. & Tang, Y. 1990. Soil-Structure Interaction effects for laterally excited liquid storage tanks. *Earthq. Eng. Struct. Dyn*. 19, 473–496.